

Control of Radial Potential Profile and Nonambipolar ion Transport in an Electron Cyclotron Resonance Mirror Plasma

著者	畠山 力三
journal or publication title	Physical review letters
volume	56
number	17
page range	1815-1818
year	1986
URL	http://hdl.handle.net/10097/35116

doi: 10.1103/PhysRevLett.56.1815

Control of Radial Potential Profile and Nonambipolar Ion Transport in an Electron Cyclotron Resonance Mirror Plasma

A. Tsushima, T. Mieno, M. Oertl,^(a) R. Hatakeyama, and N. Sato
Department of Electronic Engineering, Tohoku University, Sendai 980, Japan
 (Received 9 October 1985)

A radial profile of plasma potential is successfully controlled by the use of circular concentric segmented electrodes at both ends in a simple axisymmetric electron cyclotron resonance mirror plasma. An enhancement of radial nonambipolar ion transport is clearly observed under a condition where the ion Larmor motion is strongly modified by a radial electric field directed outward.

PACS numbers: 52.55.Jd, 52.25.Fi, 52.50.Gj

There has been an increasing interest in the role of plasma potential in magnetic plasma confinement devices, such as mirrors, stellarators, and tokamaks. Especially, it is of crucial importance in tandem mirror machines to control axial and radial profiles of plasma potential in order to attain the necessary plasma confinement for a fusion reactor.¹ It is also basically quite interesting to control plasma potential profiles and investigate plasma transport influenced by strong electric fields. Radial ion transport and its reduction by floating segmented endplates was recently reported by Simonen *et al.*² and Inutake *et al.*³ According to their results, the scaling of nonambipolar radial confinement time τ^{NA} is $\tau^{\text{NA}} \approx (3 \text{ kV}^2 \text{ ms})/\phi^2$ and $\tau^{\text{NA}} \approx (20 \text{ kV ms})/\phi$, where ϕ is the central plasma potential with respect to the grounded vacuum chamber. In the experiments, a radial electric field was considered to play an important role. But there has been no clear answer to the reason for the difference between the two works. Besides, it is difficult to measure real profiles of a radial electric field in those big machines. To know more details of the phenomena, some preliminary measurements on the potential control and related radial transport have been made in Constance B⁴ and Phaedrus⁵ experiments.

This report presents radial plasma potential profiles controlled by biasing circular concentric segmented targets at both ends in a simple axisymmetric electron cyclotron resonance (ECR) mirror plasma. We also demonstrate an enhancement of nonambipolar radial ion transport with an increase in the radial electric field directed outward.

Measurements are carried out in the straight section of the Q_T -Upgrade machine of Tohoku University, which is shown schematically in Fig. 1(a). An axial profile of the magnetic field B , also shown in Fig. 1(a), yields a magnetic field of mirror ratio 2.88. The distance between the mirror points is about 100 cm. The vacuum chamber, the diameter of which is 20.8 cm, is grounded electrically. A 6-GHz microwave with 500 W power is injected into the chamber through a waveguide situated 32.5 cm from the mirror midplane perpendicular to the chamber axis. An electron-cyclotron-resonance layer is located 20 cm from the

midplane, where $B = 2.14 \text{ kG}$. An axisymmetric plasma is produced by this resonance under Ar gas pressure of $5 \times 10^{-5} \text{ Torr}$. The plasma is terminated at targets placed at the east and west ends of the machine, as shown in Fig. 1(a). The axial distance between the targets is 140 cm. Each target consists of three circular concentric segmented electrodes [see Fig. 1(b)] whose diameters are 4, 10, and 17.5 cm, respectively. The segmented electrodes are biased at $\phi_T(\alpha/\beta/\gamma)$ in-

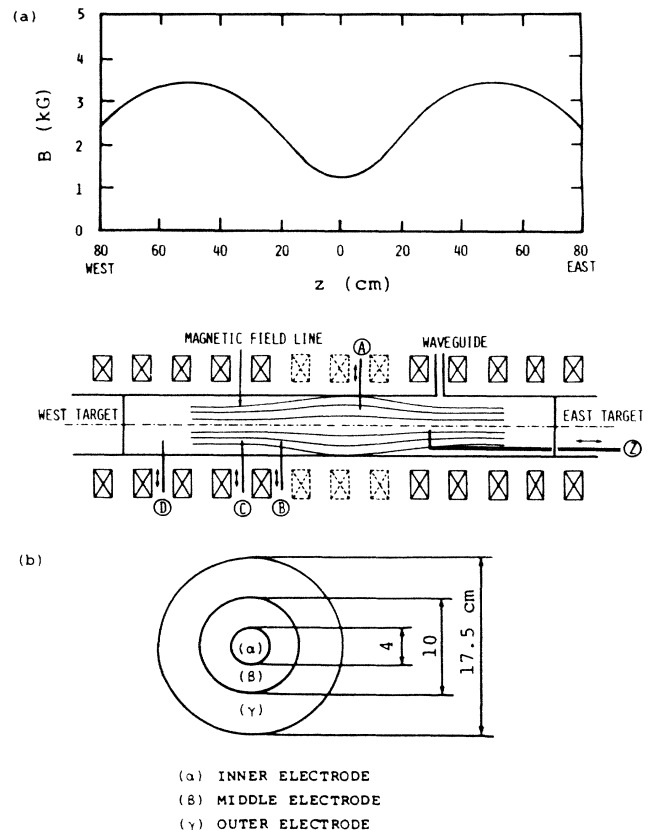


FIG. 1. (a) Schematic of experimental setup and axial profile of magnetic field B . Targets are placed at east and west ends. Small Langmuir probes, A, B, C, D, and Z, which are also used as emissive probes, are inserted radially and axially. Mirror ratio is 2.88. (b) Targets consisting of three circular concentric segmented electrodes.

dependently, where $\phi_T(\alpha/\beta/\gamma)$ represents that the bias potentials of the inner, middle, and outer electrodes are $\alpha, \beta,$ and γ V, respectively. Small movable Langmuir probes, which can be also used as emissive probes, are inserted radially and axially to measure the plasma parameters and their fluctuations.

When all of the segmented electrodes are grounded, axial and radial profiles of the plasma density n are measured as shown in Fig. 2. Around the mirror center, $n \approx 3 \times 10^{11} \text{ cm}^{-3}$, electron temperature $T_e \approx 5 \text{ eV}$, and ion temperature $T_i \leq 1 \text{ eV}$. Appreciable spatial variations of T_e and T_i are not recognized. The plasma potential ϕ is observed to change slightly in the range less than or approximately a few volts along the magnetic field. In Fig. 2, the plasma is found to be well trapped in the mirror field, being bounded by the magnetic field lines which intersect the chamber wall at the mirror midplane. Even if all of the segmented electrodes are floated (floating potentials are 1.3, 1.3, and 3.5 V for the inner, middle, and outer electrodes, respectively), the profiles of n are almost the same as in Fig. 2.

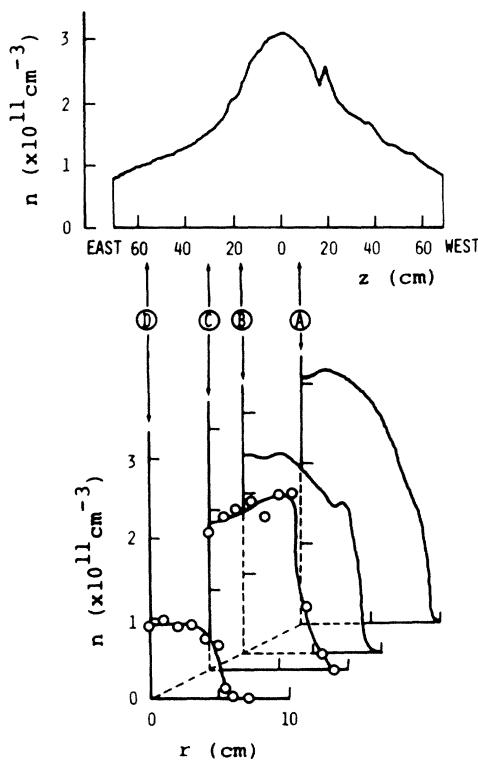


FIG. 2. Axial and radial profiles of plasma density n when all segmented electrodes are grounded electrically. Microwave power $\approx 500 \text{ W}$. Ar gas pressure $\approx 5 \times 10^{-5} \text{ Torr}$. Solid lines are obtained by measurement of ion saturation currents of Langmuir probes. Open circles show the values obtained from the characteristics of Langmuir probes. A, B, C, and D correspond to the positions of the probes in Fig. 1(a).

In order to change a radial profile of plasma potential ϕ , different bias potentials are applied to the segmented electrodes. Figure 3 demonstrates typical examples of controlled radial potential profiles and corresponding density profiles around the mirror midplane. Here the segmented electrodes are biased in the same way at both ends. Hill- and well-shaped potential profiles are found to be successfully formed. The hill-shaped potential profile is formed when the segmented electrodes are biased in the way $\alpha > \beta > \gamma$. On the other hand, the well-shaped profile is formed by the opposite combination of the bias potentials, i.e., $\alpha < \beta < \gamma$. A gradual change of the potential profile is observed between the hill- and well-shaped profiles. Even near the chamber wall, the plasma potential depends on the potential applied to the segmented electrodes. It must be remarked that $\alpha, \beta,$ and γ are

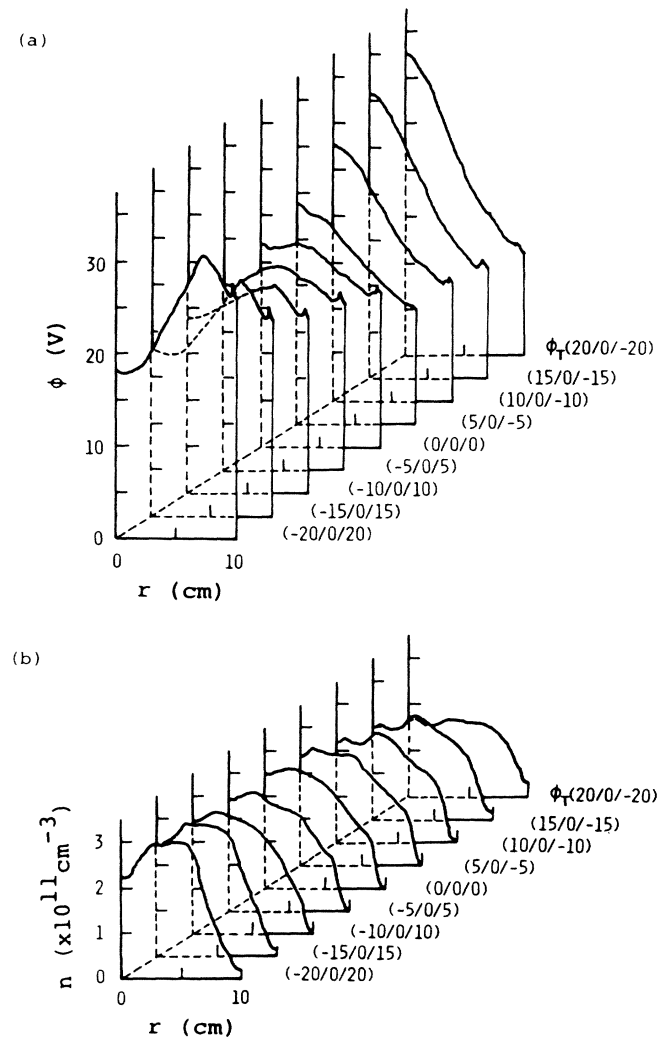


FIG. 3. (a) Controlled radial profiles of plasma potential ϕ and (b) corresponding profiles of plasma density n . $\phi_T(\alpha/\beta/\gamma)$ represents that bias potentials of inner, middle, and outer electrodes are $\alpha, \beta,$ and γ V, respectively.

always much smaller than the plasma potentials in front of the corresponding electrodes. In the case of the hill-shaped profile, n is found to decrease as the potential slope becomes steep. The result is closely related to nonambipolar ion transport mentioned below.

The measurements above suggest that the plasma is characterized by the flux tube along the magnetic field. Let us consider the plasma in the flux tube terminating at the inner electrodes at the east and west ends. Under our situation, the total electric current flowing out from the plasma inside this flux tube is always zero. Thus, a radial electric current I_r^{in} from this flux tube can be estimated by measurement of axial electric currents I_z^{in} flowing into the inner electrodes at the both ends. The same amounts of current ($I_z^{\text{in}}/2$) are measured to flow into the east and west electrodes. In Fig. 4, I_r^{in} ($= -I_z^{\text{in}}$), estimated in this way, is plotted as a function of the radial electric field E_r at a radial position $r \approx 3$ cm around the mirror midplane, where the boundary of the flux tube is located. When the radial electric field is directed inward ($E_r < 0$), I_r^{in} is negative and is found to saturate even if $|E_r|$ is increased. On the other hand, in the case of the outward electric field ($E_r > 0$), I_r^{in} increases drastically with an increase in E_r .

When E_r is positive, I_z^{in} is due to electron currents flowing into the inner electrodes at the both ends. In this case, I_r^{in} can be ascribed to a radial ion flow from the flux tube considered. This is confirmed by measurement of radial ion currents toward the wall. It is reasonable that these nonambipolar electron and ion losses result in the decrease of n for large values of E_r in Fig. 3(b). In general, the nonambipolar radial ion speed v_{ir} is represented by use of E_r and $\nabla_r n$ (radial density gradient), i.e., $v_{ir} = \mu_i E_r - D_i (\nabla_r n)/n$, where μ_i and D_i are the ion mobility and diffusion coefficient, respectively, for the nonambipolar radial ion flow, and $\mu_i = (e/T_i) D_i$ (e is the electric charge of an

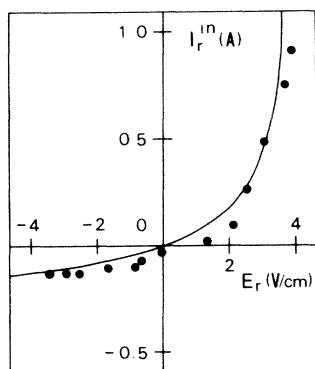


FIG. 4. A relation between radial current I_r^{in} from a flux tube terminating at inner electrodes and radial electric field E_r at the boundary of this flux tube. Closed circles show observed values. The solid line is given by Eq. (1).

ion). For the hill-shaped potential profiles in our experiment, however, $\mu_i E_r / [D_i (\nabla_r n)/n] \gg 1$ and thus $v_{ir} \approx \mu_i E_r$ at $r \approx 3$ cm. On the other hand, we have the relation $I_r^{\text{in}} \approx 2\pi a l n v_{ir}$ between I_r^{in} and v_{ir} , where a (≈ 3 cm) is the characteristic radius of the flux tube and l is the characteristic length of the plasma column, which is given to be 40 cm by the half-width of the n profile in Fig. 2(a). Thus, the ion mobility and diffusion coefficient are estimated from the measured parameters by the relation $\mu_i^{\text{expt}} = (e/T_i) D_i^{\text{expt}} \approx (I_r^{\text{in}}/E_r)/2\pi a l n$. In the case of small radial electric field ($|E_r| \leq 1.5$ V/cm), μ_i^{expt} and D_i^{expt} are roughly estimated to be $0.22 \text{ m}^2/\text{s} \cdot \text{V}$ and $0.22 \text{ m}^2/\text{s}$ ($T_i \approx 1 \text{ eV}$), respectively. Then, the effective ion collision frequency ν_i for momentum transfer is estimated from the expression given by the classical transport theory⁶ as

$$\nu_i = \mu_i^{\text{expt}} (T_i/e)/\rho_i^2 \approx 12 \times 10^3 \text{ s}^{-1},$$

where $\rho_i \approx 0.42$ cm. In our case, ν_i is mainly due to the ion production provided by ionization and the ion-neutral collisions including charge-exchange collisions, i.e., $\nu_i \approx \nu_I + \nu_c$, where ν_I and ν_c are the ionization frequency and the ion-neutral collision frequency, respectively. The value $\nu_i \approx 12 \times 10^3 \text{ s}^{-1}$ estimated roughly above is considered to be reasonable because $\nu_I \approx 4 \times 10^3 \text{ s}^{-1}$ and $\nu_c \approx 5 \times 10^3 \text{ s}^{-1}$ under our experimental condition.

When E_r is increased, however, μ_i^{expt} and D_i^{expt} are enhanced up to values five times as large as the classical values mentioned above. Small low-frequency fluctuations (≤ 10 kHz) are observed, depending on E_r , in the range of the fluctuation $\tilde{n}/n \leq 3\%$. But, there is no correlation between the fluctuation and I_r^{in} . Thus, the fluctuations are not connected with the radial ion transport observed in the experiment. For such a large electric field yielding the enhancement of radial ion transport, the ion velocity is so large that the inertia term $M \mathbf{v} \cdot \nabla \mathbf{v}$ (ion convection) cannot be neglected in the equation of ion motion. In this case, if ν_i is small, the azimuthal ion speed $v_{i\theta}$ is given by the relation

$$v_{i\theta} \approx (\omega_{ci} r/2) [-1 + (1 - 4\omega_E/\omega_{ci})^{1/2}],$$

where a parabolic radial potential $\phi \propto r^2$ is simply assumed, ω_{ci} ($= eB/M$) is the ion cyclotron frequency, and ω_E [$= E_r/(rB)$] is the precessional frequency of $\mathbf{E} \times \mathbf{B}$ drift motion. In the presence of the ion collision for momentum transfer, even if ν_i is small, the ions move radially with the speed v_{ir} expressed by

$$v_{ir} \approx (v_i r/2) [-1 + (1 - 4\omega_E/\omega_{ci})^{-1/2}]. \quad (1)$$

When $\omega_E \ll \omega_{ci}$, Eq. (1) yields the result that $\mu_i = (e/M)(v_i/\omega_{ci}^2)$ [$= (e/T_i)\rho_i^2 \nu_i$] is independent of E_r . But Eq. (1) predicts a strong dependence of μ_i on E_r for $\omega_E/\omega_{ci} \geq 0.1$ which corresponds to the observed

criterion $E_r \geq 2$ V/cm in our experiment. Substituting $\nu_i \approx 12 \times 10^3$ s⁻¹ in Eq. (1), we can calculate I_r^{in} ($= 2\pi r l e n v_{ir}$) at $r = a$, which is shown by a solid line in Fig. 4. It can be found that the result is quite consistent with the observed values of I_r^{in} , showing the importance of the ion convection for radial ion transport in our case.

In an ECR plasma, there is no electric current associated with plasma production and electric currents are always caused by nonambipolar particle transport. This situation is suitable for experimental investigation of plasma transport. We have demonstrated measurements of controlled potential profiles and related ion transport in a simple axisymmetric ECR mirror plasma. The radial slope of a hill-shaped potential profile has been shown to be successfully controlled, and even a well-shaped profile has been realized, by adjustment of the bias potentials applied to the circular concentric segmented targets at both ends of the machine. The result is the first demonstration of such a drastic control of radial plasma potential profile. A main difference between our experiment and the previous tandem-mirror experiments might be that a relatively high-density plasma is in contact with the targets, providing a better line-tying mechanism, in our experiment. In fact, the potential change is observed to become large with a decrease in R_m . An enhancement of the nonambipolar radial ion transport has also been clearly observed by increasing radial electric field directed outward. This enhancement is due to the ion

convection under a strong radial electric field. The phenomenon is quite interesting in the consideration of plasma transport and is also of significant importance in future fusion research.

We express our gratitude to M. Inutake for his helpful discussions, and to H. Ikegami and M. Fujiwara for their interest in this work. We are indebted to K. Saeki and A. Komori for their collaboration in the construction of the Q_T -Upgrade machine of Tohoku University. We also thank H. Ishida and Y. Takahashi for their technical assistance.

(a)Present address: Institute for Theoretical Physics, University of Innsbruck, A-6020 Innsbruck, Austria.

¹G. I. Dimov *et al.*, *Fiz. Plasmy* **2**, 597 (1976) [*Sov. J. Plasma Phys.* **2**, 326 (1976)]; T. K. Fowler and B. G. Logan, *Comments Plasma Phys. Controlled Fusion* **2**, 167 (1977); D. E. Baldwin and B. G. Logan, *Phys. Rev. Lett.* **43**, 1318 (1979); E. B. Hooper *et al.* *Phys. Fluids* **27**, 2264 (1984).

²T. C. Simonen *et al.*, in *Proceedings of the Tenth International Conference on Plasma Physics and Controlled Nuclear Fusion Research, London, 1984* (International Atomic Energy Agency, Vienna, 1985), Vol. 2, p. 255.

³M. Inutake *et al.*, *Phys. Rev. Lett.* **55**, 939 (1985).

⁴D. K. Liu *et al.*, *Bull. Am. Phys. Soc.* **29**, 1270 (1984).

⁵N. Hershkowitz *et al.*, in Ref. 2, p. 265.

⁶S. I. Braginskii, in *Review of Plasma Physics*, edited by M. A. Leontovich (Consultants Bureau, New York, 1965), Vol. 1, p. 205.